ISSN 1070-3284, Russian Journal of Coordination Chemistry, 2009, Vol. 35, No. 10, pp. 731–739. © Pleiades Publishing, Ltd., 2009.
Original Russian Text © V.V. Gorinchoy, V.E. Zubareva, S.G. Shova, V.N. Szafranski, J. Lipkowski, N. Stanica, Yu.A. Simonov, C.I. Turta, 2009, published in Koordinatsionnaya Khimiya, 2009, Vol. 35, No. 10, pp. 743–751.

Homo- and Heteronuclear Iron Complexes {Fe_2MO} with Salicylic Acid: Synthesis, Structures, and Physicochemical Properties

V. V. Gorinchoy[a], V. E. Zubareva[a], S. G. Shova[b], V. N. Szafranski[a], J. Lipkowski[c], N. Stanica[d], Yu. A. Simonov[b], and C. I. Turta[a]*

[a] *Institute of Chemistry, Academy of Sciences of Moldova, Chisinau, Moldova*
[b] *Institute of Applied Physics, Academy of Sciences of Moldova, Chisinau, Moldova*
[c] *Institute of Physical Chemistry, Polish Academy of Sciences, Warsaw, Poland*
[d] *Institute of Physical Chemistry, Romanian Academy of Sciences, Bucharest, Romania*
**e-mail: turtac@yahoo.com*

Received December 17, 2008

Abstract—A reaction of iron nitrate with magnesium salicylate and reactions of iron and cobalt chlorides with ammonium salicylate in the presence of water, methanol, DMAA, and DMF gave the trinuclear heterometallic complexes: [hexa-μ-salicylato-μ_3-oxo-0.4-dimethylacetamide-2.6-aquadiiron(III)magnesium(II)] tetra(dimethylacetamide), $[Fe_2MgO(SalH)_6(DMAA)_{0.4}(H_2O)_{2.6}] \cdot 4DMAA$ (**I**); [hexa-μ]-salicylato-μ_3-oxo(dimethanol)aquadiiron(III)cobalt(II)] dimethylformamide · 2.5-hydrate, $[Fe_2CoO(SalH)_6(CH_3OH)_2(H_2O)] \cdot DMF \cdot 2.5H_2O$ (**II**); and [hexa-μ-salicylato-μ_3-oxotriaquatriiron(III)] chloride dimethylacetamide monohydrate, $[Fe_3O(SalH)_6(H_2O)_3]Cl \cdot DMAA \cdot H_2O$ (**III**). The X-ray study revealed that the molecular structures of complexes **I** and **II** are $[Fe_2^{III}M^{II}(\mu_3\text{-}O)(RCOO)_6L_3] \cdot n$Solv. The IR and Mössbauer spectra of complexes **I**–**III** were examined; their magnetochemical and thermal properties were studied. The parameters of the Mössbauer spectra ($\delta_{Na^+} = 0.69 \pm 0.03$ mm/s, $\Delta E_Q = 0.76\text{–}1.08$ mm/s, 300 K) suggest the high-spin state of the Fe^{3+} ions in complexes **I**–**III** ($S = 5/2$). The paramagnetic Fe^{3+} ions are involved in antiferromagnetic exchange interactions with the parameter $J = -44$ cm^{-1}, $g = 2.05$ (for **I**). Complexes **I**–**III** are thermally unstable.

DOI: 10.1134/S1070328409100042

The chemistry of homo- and heteropolynuclear iron carboxylates are of current interest because they help the researchers to enhance their knowledge of magnetic interactions between paramagnetic ions [1] and promote the development of bioinorganic chemistry [2]. Compounds of this class serve as precursors of nanooxide and metallic particles with useful magnetic properties [3] and can be used as physiologically active drugs [4], etc.

Metal complexes with acetic acid [5] and its halogen derivatives [6–12] have been comprehensively studied to date. The structures of many such complexes were proved by X-ray diffraction. Some studies were devoted to the structures and properties of complexes with hydroxy carboxylic acids (e.g., salicylic acid, H_2Sal). According to the literature data, coordinated salicylic acid is fully or partially deprotonated and can act as a monodentate, chelating bidentate, or bridging ligand [13]. For instance, salicylic acid in a dimeric terbium complex has been found to be coordinated in three ways [14]. In a nanonuclear manganese complex with benzoic and salicylic acids, the anion Sal^{2-} is coordinated in a pentadentate chelating μ_3-bridging fashion [15]. Among 120 metal complexes with salicylic acid deposited with the Cambridge Crystallographic Data Collection, we have found no iron(III) μ_3-oxo salicylates [16].

In this study, we obtained the trinuclear homo- and heterometallic iron(III) complexes $[Fe_2MgO(SalH)_6(DMAA)_{0.4}(H_2O)_{2.6}] \cdot 4DMAA$ (**I**), $[Fe_2CoO(SalH)_6(CH_3OH)_2(H_2O)] \cdot DMF \cdot 2.5H_2O$ (**II**), and $[Fe_3O(SalH)_6(H_2O)_3]Cl \cdot DMAA \cdot H_2O$ (**III**) and examined their structures.

EXPERIMENTAL

The starting salt $Mg(SalH)_2 \cdot 3H_2O$ was prepared from MgO and salicylic acid. The other reagents (CH_3OH, DMAA, DMF, and THF) were commercial chemicals.

Synthesis of complex I. The salt $Mg(C_6H_4(OH)COO)_2 \cdot 3H_2O$ (3.49 g, 9.89 mmol) was added with continuous stirring to $Fe(NO_3)_3 \cdot 9H_2O$ (1 g, 2.47 mmol) in methanol (25 ml). After 30 min, the resulting solution was filtered and dried on a water bath. To a dry residue THF (18 ml) and DMAA (7 ml) were added. The mixture was stirred at room temperature for 20 min, filtered, and left in air for crystallization. After four weeks, dark red crystals of complex **I** formed as rectangular prisms. The yield was 2.72 g (69%).

For $C_{59.6}H_{74.8}Fe_2MgN_{4.4}O_{26}$

anal. calc., %:	C, 50.95;	H, 5.36;	N, 4.38.
Found, %:	C, 50.78;	H, 5.47;	N, 4.43.

Synthesis of complex II. A solution of $CoCl_2 \cdot 6H_2O$ (1.15 g, 4.8 mmol) in methanol (10 ml) was added to ammonium salicylate (1.5 g, 9.68 mmol) in methanol (10 ml). The mixture was refluxed for ~1 h, whereupon a solution of $Fe(NO_3)_3 \cdot 9H_2O$ (0.49 g, 1.2 mmol) in a mixture of methanol (10 ml) and DMF (1 ml) was added. Heating was continued while stirring the mixture until pink flakes dissolved completely. After 1 h, DMF (1 ml) and THF (1 ml) were added. This resulted in the formation of a fine crystalline solid, which dissolved completely on 1-h heating. The resulting dark red solution was transferred to a warm beaker and left for crystallization. After a day, a dark brown (with a reddish tinge) coarse crystalline solid was filtered off, washed with methanol (2 ml) and ether (2 ml) (the solid is soluble in both solvents), and dried in air. Single crystals suitable for X-ray diffraction analysis were obtained by recrystallization of complex **II** from methanol. The yield was 0.51 g (68%).

For$C_{47}H_{52}CoFe_2NO_{25.5}$

anal. calcd, %:	C, 46.67;	H, 4.33;	N, 1.15.
Found, %:	C, 45.77;	H, 4.20;	N, 1.46.

Synthesis of complex III. A solution of $FeCl_3 \cdot 6H_2O$ (1 g, 2.7 mmol) in methanol (4 ml) and a solution of ammonium salicylate (1.15 g, 7.4 mmol) in methanol (5 ml) were mixed to give a dark violet precipitate. The precipitate was stirred with DMAA (0.8 ml, 9.2 mmol). A fine crystalline red-brown solid formed. Water (10 ml) was added and the reaction mixture was thoroughly stirred. The product was filtered off and washed with water (2 × (15–20) ml). The yield was 1.1 g (25%).

For $C_{46}H_{47}ClFe_3NO_{24}$

anal. calcd, %:	C, 46.01;	H, 3.94;	N, 1.17.
Found, %:	C, 45.85;	H,4.27;	N, 1.18.

Complexes **I**–**III** were analyzed for C, H, and N by the elemental analysis group of the Institute of Chemistry of the Academy of Sciences of the Moldova Republic. Complexes **I**–**III** were analyzed for metals on an AAS-1N atomic absorption spectrometer (Carl Zeiss) at the Center of Metrology and Analytical Methods of the Academy of Sciences of the Moldova Republic.

X-ray diffraction analysis. Experimental material for complexes **I** and **II** was collected at 100 K on a Nonius Kappa CCD diffractometer (MoK_α radiation, graphite monochromator, ω–2θ scan mode). The unit cell parameters were refined for the whole array of experimental data. The integration of the reflection intensities and their reduction to a common scale was performed with the DENZO and SKALEPACK programs [17]. Absorption correction was applied with the XEMP program [18].

Structures **I** and **II** were solved by direct methods and refined by the least-squares method in the anisotropic full-matrix approximation for non-hydrogen atoms (SHELX-97) [19]. The hydrogen atoms in complex **I** were located objectively; those in complex **II** were calculated geometrically and refined isotropically using the rigid-body model. The refinement revealed that the position at the M(2) atom in complex **I** is randomly occupied by water and DMAA molecules (0.6 : 0.4). In complex **II**, the hydroxy O atoms of the coordinated HSal residues are disordered.

Crystallographic parameters and the data collection statistics for structures **I** and **II** are given in Table 1. Selected bond lengths and bond angles are listed in Tables 2 and 3. Atomic coordinates and other parameters for structures **I** and **II** have been deposited with the Cambridge Crystallographic Data Collection (nos. 723904 (**I**) and 723 903 (**II**)); deposit@ccdc.cam.ac.uk or http://www.ccdc.cam.ac.uk/data_request/cif.

IR spectra were recorded on a Specord M75 spectrometer in the 200–600 cm^{-1} range and a Perkin-Elmer 100 FT-IR spectrometer in the 400–4000 cm^{-1} range (suspensions in Vaseline or fluorinated oils).

Integrated thermal analysis was carried out on a Paulik–Paulik–Erdey derivatograph in air with Al_2O_3 as a reference. The recording conditions were 1/5 (DTG), 1/10 (DTA), and 100/100 (TG), $T_{max} = 800°C$, heating rate 5°C/min, a sample weight 100 mg.

The magnetic properties of complexes **II** and **II** were studied by the Gouy method at room temperature; the temperature range for complex **I** was 291–136 K. The magnetic susceptibility was calibrated against $Hg[Co(NCS)_4]$. Diamagnetic corrections were applied from the Pascal constants [1, 20].

Mössbauer spectra were recorded on an electrodynamic setup with a constant acceleration at room temperature; ^{57}Co in a Rh matrix was used as a radiation source (1.0 MBq). The isomer shifts are referenced to sodium nitroprusside.

RESULTS AND DISCUSSION

Heterotrinuclear iron complexes with salicylic acid can be obtained when mixing a solution of iron(III) nitrate with some metal salicylate, or with simple metal salts in the presence of ammonium salicylate. It was found that the formation of a crystalline product is well

Table 1. Crystallographic parameters and the data collection statistics for structures **I** and **II**

Parameter	Value	
	I	**II**
M	1404.85	1209.53
Space group	$C2/c$	$C2/c$
Unit cell parameters		
a, Å	43.3859(15)	13.4150(3)
b, Å	15.3037(5)	21.0090(6)
c, Å	20.8776(6)	21.5450(5)
β, deg	103.997(3)	99.920(2)
V, Å^3	13450.4(7)	5981.4(3)
Z	8	4
ρ_{calcd}, g/cm^3	1.388	1.343
μ_{Mo}, mm^{-1}	0.524	0.830
F(000)	5882	2496
θ scan range, deg	2.01–26.00	1.82–26.00
(Ranges of h, k, and l indices	$-53 \le h \le 53, -18 \le k \le 18, -25 \le l \le 25$	$-16 \le h \le 16, -25 \le k \le 25, -26 \le l \le 26$
Number of measured reflections:	98644	11078
Number of independent reflections, $I > 2\sigma(I)$	13205 ($R_{int} = 0.0846$)	5858 ($R_{int} = 0.0627$)
Completeness of data collection for θ, %	99.9	99.5
Number of parameters refined	1032	388
GOOF on F_2	1.129	1.038
R factors ($I > 2\sigma(I)$)	$R_1 = 0.0751$, $wR_2 = 0.2199$	$R_1 = 0.0997$, $wR_2 = 0.2663$
R factors (for all reflections)	$R_1 = 0.1423$, $wR_2 = 0.2584$	$R_1 = 0.1398$, $wR_2 = 0.2889$
$\Delta\rho_{max}$ and $\Delta\rho_{min}$, e Å^{-3}	0.703 and –0.929	1.264 and –0.462

reproducible only in the presence of a small amount of dimethylacetamide. In addition, a considerable excess of bivalent metal ions (Mg^{2+} and Co^{2+}) is required to incorporate them into a trimer structure.

The best results were obtained in the study of reactions of Fe^{3+} ions with salicylates of other 2s- and 3d metals (Mg or Co) in the CH_3OH–DMAA–THF system. In this series of solvents, the affinity for coordination changes as follows: THF < DMAA ~ DMF < H_2O ~ CH_3OH.

Structures **I** and **II** are molecular ones. The trinuclear complexes $[Fe_2MO(OOCR)_6 \cdot 3L] \cdot n$Solv contain two iron(III) atoms and a bivalent metal atom (M = Mg (**I**, Fig. 1) and Co (**II**, Fig. 2)). The outer sphere in the packing of large trinuclear complexes in the crystal space is made up of solvate molecules (nSolv = 4DMAA (**I**) and DMF · 2.5H_2O (**II**)).

A main problem in the study of trinuclear heterometallic complexes is the determination of the distribution of metal cations in the cluster. Their statistical distribution was proved in [21–24]. In some cases [25–27] (e.g., for close atomic numbers of the metal cations in the Periodic Table), such a distribution is presumed. In other cases, a statistical distribution of cations follows from the own symmetry of complex C_3 [28]. In recent years, localization of foreign cations has been proved for trimers containing metals with different atomic radii, electronic properties, and atomic numbers in the Periodic Table. This fact was revealed with Fe_2/Sr, Fe_2/Ba, and Fe_2/Ca complexes of the formula $[Fe_2M(Ca,Sr,Ba)O(CCl_3COO)_6(THF)_n]$ [29]. The differences between the ionic radii of Fe^{3+} (0.78 Å), Ca^{2+} (1.00 Å), Sr^{2+} (1.18 Å), and Ba^{2+} (1.35 Å) make the M_3 triangle substantially distorted. In physicochemical characteristics, magnesium is an analog of calcium, strontium, and barium, but its ionic radius (0.72 Å [30]) is sufficiently close to that of iron(III); therefore, one can expect its incorporation into the M_3 triangle in complex **I**.

In [24], it was found that the Mg^{2+} ions in $[Fe_2^{III}Mg^{II}O(OCl_3COO)_6Py_3] \cdot CH_3C_6H_5$ (**IV**) are statistically distributed with iron atoms over two positions of the trimer and those in $[Fe_2^{III}Mg^{II}O(OCl_3COO)_6(THF)_3]$ are statistically distributed over all three positions. Such a distribution is also true for metal–ligand distances in coordination entities. In complex **I**, the M–M distances in the triangle are 3.288–3.234 Å and the M–O distances are normal for complexes of this type (Table 2). It is impossible to identify the positions predominantly occupied by Mg or Fe atoms. An analysis of the geometrical parameters did not reveal the dominant occupation of the positions M(1)–M(3) by Fe^{3+} and Mg^{2+} cations. In crystal structure **I**, the geometry of the triangle M(3)(μ_3-O) is typical. Each metal atom has a slightly distorted octahedral environment with close interatomic distances and geometrical parameters. The average M–$O(1)_{oxo}$ (1.887 Å) and M–O_{carb} bond lengths (2.036 Å) in complex **I** do not differ substantially from those in complex **IV**. The specific feature of

Table 2. Selected bond lengths and bond angles in structure **I**

Bond	*d*, Å	Bond	*d*, Å	Bond	*d*, Å
M(1)–O(1)	1.919(3)	M(2)–O(1)	1.880(3)	M(3)–O(1)	1.862(3)
M(1)–O(1*w*)	2.093(4)	M(2)–O(2*w*)	2.116(3)	M(3)–O(3)	2.034(4)
M(1)–O(2)	2.043(3)	M(2)–O(7)	2.041(4)	M(3)–O(5)	2.030(3)
M(1)–O(4)	2.028(4)	M(2)–O(9)	2.047(3)	M(3)–O(11)	2.036(4)
M(1)–O(6)	2.039(4)	M(2)–O(10)	2.031(3)	M(3)–O(13)	2.027(3)
M(1)–O(8)	2.050(3)	M(2)–O(12)	2.024(3)	M(3)–O(3*w*)	2.086(3)
M(1)–M(2)	3.288(1)	M(2)–M(3)	3.234(1)		
M(1)–M(3)	3.281(1)				
Angle	ω, deg	Angle	ω, deg	Angle	ω, deg
O(1)M(1)O(1*w*)	179.04(1)	O(1)M(2)O(2*w*)	177.48(1)	O(1)M(3)O(3*w*)	178.42(1)
O(1)M(1)O(2)	96.76(1)	O(1)M(2)O(7)	99.27(1)	O(1)M(3)O(3)	97.10(1)
O(1)M(1)O(4)	92.88(13)	O(1)M(2)O(9)	94.57(1)	O(1)M(3)O(5)	95.05(1)
O(1)M(1)O(6)	93.96(1)	O(1)M(2)O(10)	97.15(1)	O(1)M(3)O(11)	96.36(1)
O(1)M(1)O(8)	95.98(1)	O(1)M(2)O(12)	93.96(1)	O(1)M(3)O(13)	96.33(1)
O(2)M(1)O(1*w*)	82.29(1)	O(7)M(2)O(2*w*)	83.25(1)	O(3)M(3)O(3*w*)	84.33(1)
O(2)M(1)O(8)	167.04(1)	O(7)M(2)O(9)	88.96(1)	O(3)M(3)O(11)	166.54(1)
O(4)M(1)O(1*w*)	87.19(1)	O(9)M(2)O(2*w*)	85.32(1)	O(5)M(3)O(3)	90.65(1)
O(4)M(1)O(2)	92.31(1)	O(10)M(2)O(2*w*)	80.33(1)	O(5)M(3)O(11)	88.35(1)
O(4)M(1)O(6)	173.12(1)	O(10)M(2)O(7)	162.89(1)	O(11)M(3)O(3*w*)	82.21(1)
O(4)M(1)O(8)	89.41(1)	O(10)M(2)O(9)	84.97(1)	O(13)M(3)O(3*w*)	84.39(1)
O(6)M(1)O(1*w*)	85.98(1)	O(12)M(2)O(2*w*)	86.22(1)	O(13)M(3)O(3)	87.04(1)
O(6)M(1)O(2)	87.60(1)	O(12)M(2)O(7)	88.24(1)	O(13)M(3)O(5)	168.58(1)
O(6)M(1)O(8)	89.16(1)	O(12)M(2)O(9)	171.35(1)	O(13)M(3)O(11)	91.30(1)
O(8)M(1)O(1*w*)	84.97(1)	O(12)M(2)O(10)	95.41(1)	O(3*w*)M(3)O(5)	84.25(1)

the trimer is the statistic distribution of neutral ligands. The positions at the M(1) and M(2) atoms are unambiguously occupied by a water molecule, while the position at the M(3) atom is statistically occupied by water and DMAA molecules (0.6 : 0.4). In crystal structure **I**, the outer-sphere DMAA molecules and the complex molecules are united through a system of hydrogen bonds (Table 4). The complexes are also linked by π–π and C–H···π interactions.

Structure **II** is similar to structure **I**; the own symmetries of the trimers differ. Two Fe^{3+} ions and a Co^{2+} ion are statistically distributed, making up an isosceles triangle (M(1)–M(2), 3.287 Å; M(2)–M(3), 3.287 Å). The center of the triangle is occupied by the μ_3-O atom coplanar with the metal atoms (M(1)–O(1), 1.884 Å; M(2)–O(1), 1.895 Å). In the crystal, the M(1) and μ_3-O atoms are on the axis 2. The structure of the complex as a whole, as well as its geometrical parameters (Table 3), agrees with the literature data for related complexes [31, 32].

Each metal atom in complex **II** has an octahedral coordination but a different environment. The coordination sphere of each metal atom is built from four O atoms of the carboxyl groups and the central atom μ_3-oxo. The sixth (apical) position is occupied by a methanol molecule for M(2) and a water molecule for M(1). The average M(1)–O_{carb} and M(2)–O_{carb} bond lengths do not differ substantially, which is due to the close ionic radii of Co^{2+} (0.75 Å) and Fe^{3+} (0.78 Å) [30]. When solving structure **II**, we found that the salicylic acid residue and DMF molecules are randomly disordered. For the salicylate fragments, these two positions correlate with a rotation about the C–C_{carb} bond through 180°. Solvated DMF molecules are distributed with an equal probability between two positions about axis 2. Crystal structure **II** is primarily stabilized by intermolecular π–π stacking and, to a less degree, by O–H···O hydrogen bonding (Table 4) between water molecules and the O atoms of DMF molecules. In crystal structure **II**, infinite chains of trinuclear complexes are aligned with the crystallographic axis *z* (Fig. 3).

The presence of π–π interactions in 1D chains is confirmed by short distances (3.82 and 3.98 Å) between the centers of the aromatic rings in the antiparallel orientation. The π–π interactions of other salicylic acid residues with solvated DMF molecules unite the aforementioned chains into 2D layers parallel to the crystallographic plane *xz* (Fig. 3).

Table 3. Selected bond lengths and bond angles in structure **II***

Bond	d, Å	Bond	d, Å
M(1)–O(1)	1.884(6)	M(2)–O(1)	1.895(3)
M(1)–O(1w)	2.098(8)	M(2)–O(2)	2.066(5)
M(1)–O(3)	2.034(5)	M(2)–O(5)^1	2.030(5)
M(1)–O(8)	2.060(5)	M(2)–O(6)	2.082(5)
M(1)–M(2)	3.271(3)	M(2)–O(9)	2.039(5)
		M(2)–O(11)	2.092(5)
		M(2)–M(3)	3.287(3)
Angle	**ω, deg**	**Angle**	**ω, deg**
O(1w)M(1)O(3)	84.7(1)	O(1)M(2)O(2)	96.4(2)
O(1w)M(1)O(8)	84.6(1)	O(1)M(2)O(5)^1	94.9(2)
O(1)M(1)O(3)	95.3(1)	O(1)M(2)O(6)	94.7(2)
O(1)M(1)O(8)	95.4(2)	O(1)M(2)O(9)	95.0(2)
O(3)M(1)O(3)^1	169.4(3)	O(1)M(2)O(11)	177.5(2)
O(3)M(1)O(8)	89.6(2)	O(2)M(2)O(5)^1	89.4(2)
O(3)M(1)O(8)^1	89.5(2)	O(2)M(2)O(6)	168.8(2)
O(8)M(1)O(8)^1	169.2(3)	O(2)M(2)O(9)	88.7(2)
		O(2)M(2)O(11)	86.2(2)
		O(6)M(2)O(5)^1	91.9(2)
		O(6)M(2)O(9)	88.1(2)
		O(6)M(2)O(11)	82.8(2)
		O(9)M(2)O(5)^1	170.1(2)
		O(9)M(2)O(11)	84.8(2)
		O(11)M(2)O(5)^1	85.4(2)

* The symmetry operation code is: ^{1} $-x, y, -z + 0.5$.

Complexes **I**–**III** are characterized by complicated IR spectra. Intense absorption bands at 3600 and 3200 cm^{-1} in the IR spectra of all complexes are due to water molecules. The SalH$^-$ anion is coordinated in a bridging bidentate fashion: the band ν(CO) at 1660 cm^{-1} due to the carboxy group COOH disappears, while two bands appear at 1590–1583 (ν_{as}(COO)) and 1388–1385 cm^{-1} (ν_s(COO)) [33]. The frequency ν(C=O)(1626–1622 cm^{-1}) of the outer-sphere DMAA molecules indicates the hydrogen bonding between the carbonyl group and water molecules.

According to thermal analysis data, complexes **I**–**III** are unstable. Their thermolysis (> 50°C) involves many steps and is similar for all complexes, although with some individual features. Let us dwell on the thermal analysis data for complex **I**. The DTG and TG curves suggest the first three endothermic processes at 40–120, 120–155, and 155–235°C. The corresponding weight losses are ~12–13, 19, and 42%. From the data obtained and the composition of the complex, it seems to be highly probable that the observed changes are attributable to the sequential elimination of (2.6H_2O + 0.4DMAA), (DMAA), and (3DMAA). Subsequent exothermic processes at 235–280, 280–360, and 360–450°C are due to the elimination of all remaining organic ligands and the formation of products with atmospheric oxygen. The final thermolysis product is ~13% of the initial weight, which corresponds to the mixed oxide $Fe_2O_3 \cdot MgO$ (calculated: 14.23%).

The Mössbauer spectra of complexes **I**–**III** at 300 and 80 K show a doublet, its peaks being approximately equal in intensity; no additional absorption is detected (Fig. 4). At 80°C, the spectral pattern remains unchanged; the parameters of the Mössbauer spectra (Table 5) are typical of high-spin iron(III) complexes ($S = 5/2$).

Replacement of one iron(III) ion in the triangle by a cobalt(II) or magnesium(II) ion increases the quadrupole splitting from 0.76 to 1.08 mm/s (by ~26%). This change is consistent with our data [24, 28, 29, 34] and the data obtained by other researchers [35–38] and is due to the lowering of the symmetry of the fragment {Fe_2MO} in the complex from D_{3h} to C_{2v}. A comparison of the parameters of the Mössbauer spectra of the cobalt-containing clusters reveals a slight increase in the quadrupole splitting (0.88 $\longrightarrow$ 1.04 mm/s) when the acetate ion is replaced by a salicylate one, probably because of the ligand contribution (Table 5).

With a decrease in the temperature, the isomer shift increases by 0.13–0.15 mm/s, which agrees with the literature data for ^{57}Fe [39]. This decrease reflects a

Table 4. Parameters of the hydrogen bonds in structures **I** and **II**

D–H···A	Distance, Å			Angle DHA, deg	Symmetry operation code for A
	D–H	H···A	D···A		
			I		
O(1w)–H···O(3w)	0.91	1.83	2.62(2)	144	x, y, z
O(11)–H···O(4w)	0.97	1.65	2.59(1)	160	x, y, z
			II		
O(2w)–H···O(22)	0.89	1.78	2.67(1)	176	$0.5 - x, 0.5 - y, 1 - z$
O(3w)–H···O(24)	0.90	1.87	2.58(2)	135	$x, 1 + y, z$
O(3w)–H···O(23)	0.90	1.80	2.62(1)	151	$0.5 - x, 0.75 - y, 1 - z$

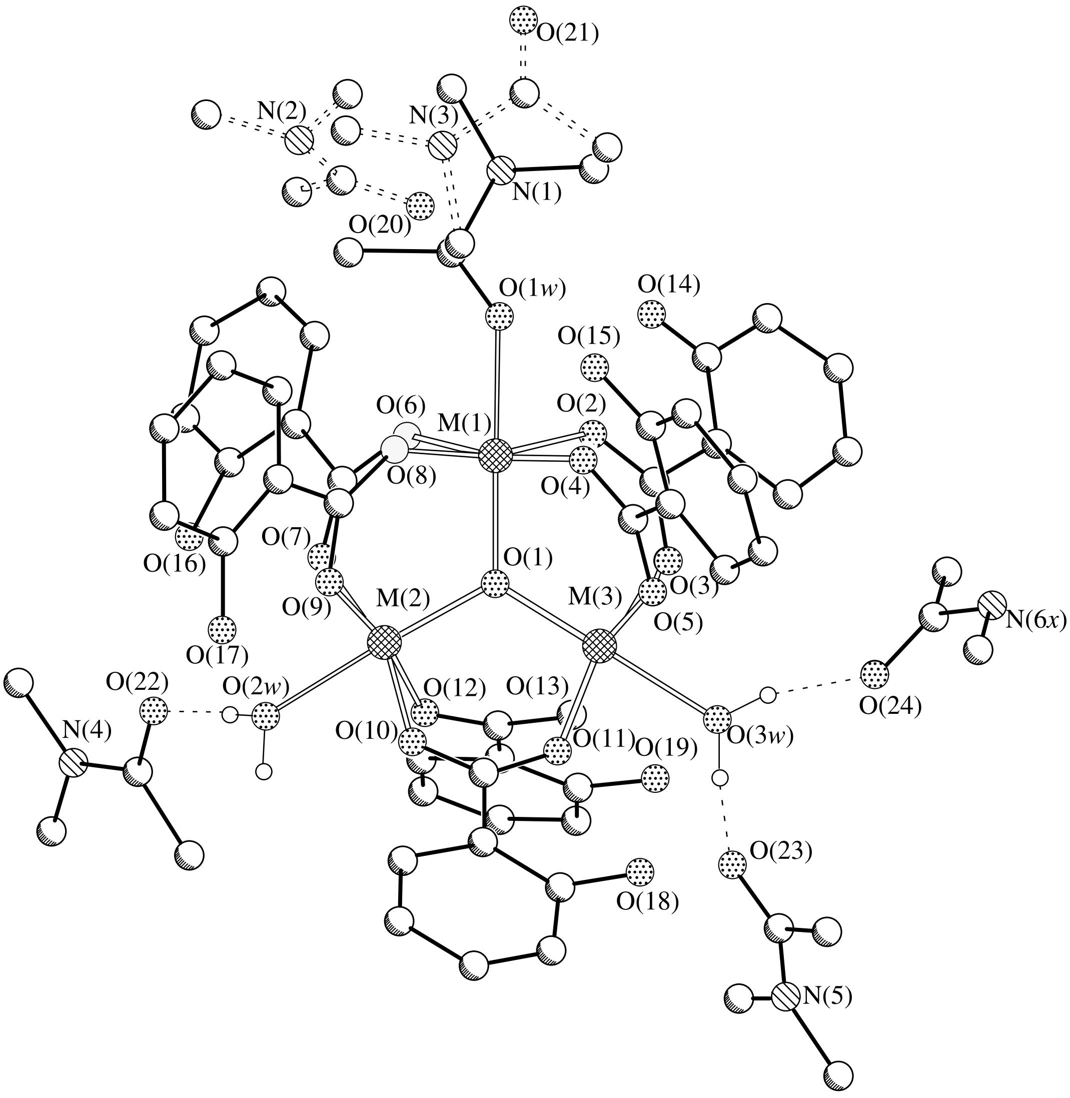

Fig. 1. Molecular structure of the complex $[Fe_2MgO(SalH)_6(DMAA)_{0.4}(H_2O)_{2.6}] \cdot 4DMAA$.

changed total *s*-electron density around the Mössbauer nucleus as a result of the second-order Doppler effect [40, 41].

The magnetic properties of complexes **I**–**III** were measured in the 291–136 K range for **I** and at room temperature for **II** and **III**. The products of the experimental values ($\chi_M T$) for complexes **I**, **II**, and **III** at room temperature are 2.24, 4.59, and 5.12 cm^3 K/mol, respectively. These are substantially lower than the products expected for non-interacting trinuclear complexes with the set of paramagnetic ions under study (8.75, 9.13, and 13.13 cm^3 K/mol, respectively). For complex **I**, $\chi_M T$ decreases from 2.24 (291 K) to 0.93 cm^3 K/mol (136 K) (Table 6). The temperature dependence of the magnetic properties of complex **I** was described in terms of the HDVV model [1, 20, 42] with the Hamiltonian of spin-spin coupling $H = -2J_{12}(\boldsymbol{S}_1 \cdot \boldsymbol{S}_2)$. The resulting parameters ($J_{Fe–Fe} \approx -44\ cm^{-1}$, $g = 2.05$, the sum of the least squares 2.66×10^{-4}) suggest an antiferromagnetic exchange interaction between the paramagnetic ions. The exchange parameter for complex **I** lies in the *J* range characteristic of other heteronuclear μ_3-oxo iron complexes with a diamagnetic heteroatom [28].

Our study confirmed that the three-center system in the clusters $[Fe_2^{III}M^{II}O(RCOO)_6 \cdot 3L]$ is stable and is found in complexes where M^{II} is a transition metal (donor-acceptor M–O bonds) and an alkaline-earth metal (ionic M–O bonds).

Introduction of a heteroatom into the metal triangle lowers the symmetry of the electron cloud around the iron nuclei. With an *s* element as a heteroatom, the antiferromagnetic exchange interaction between two Fe^{3+} ions is stronger than that in homotrinuclear clusters.

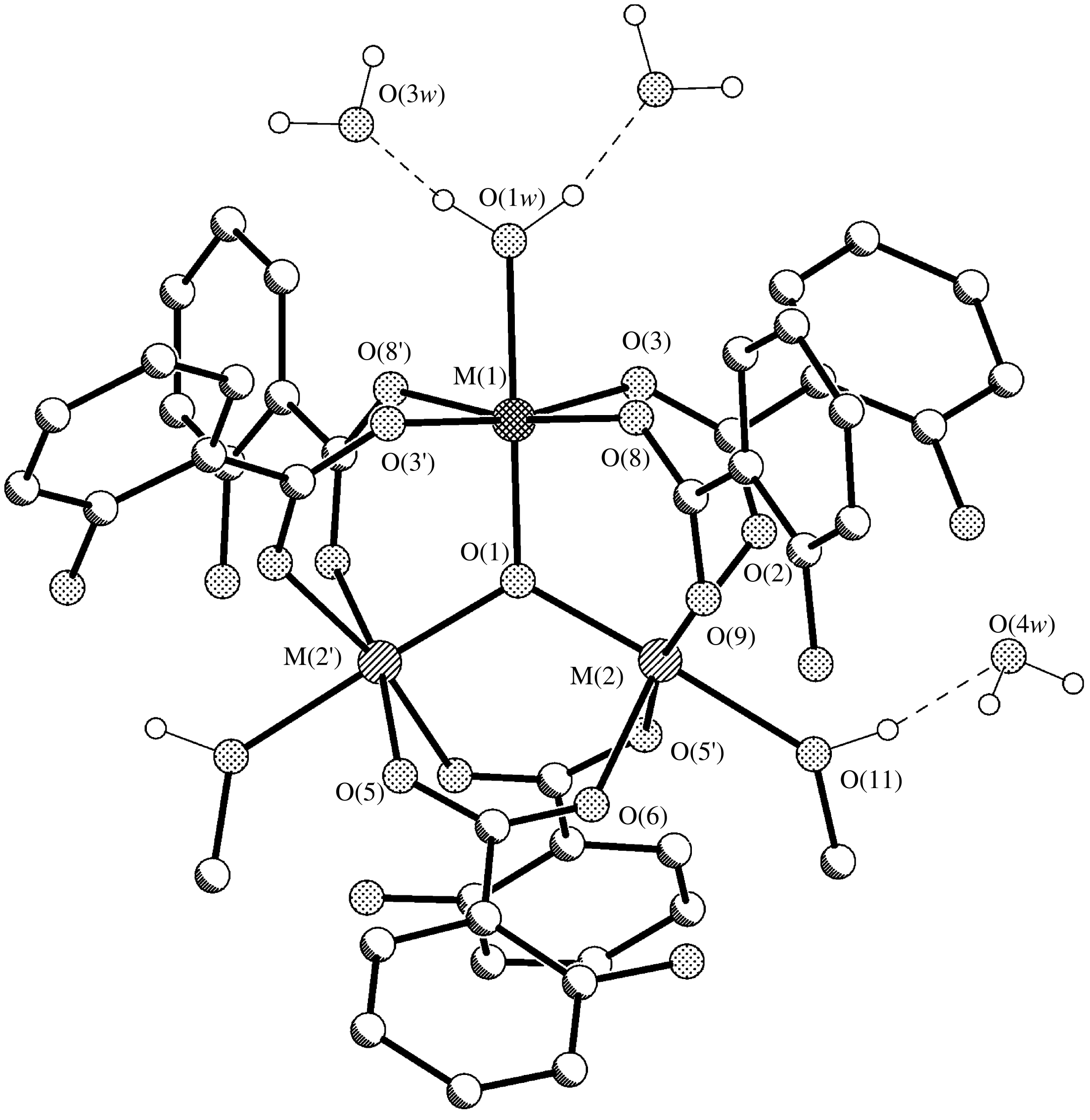

Fig. 2. Molecular structure of the complex $[Fe_2CoO(SalH)_6(CH_3OH)_2(H_2O)] \cdot DMF \cdot 2.5H_2O$.

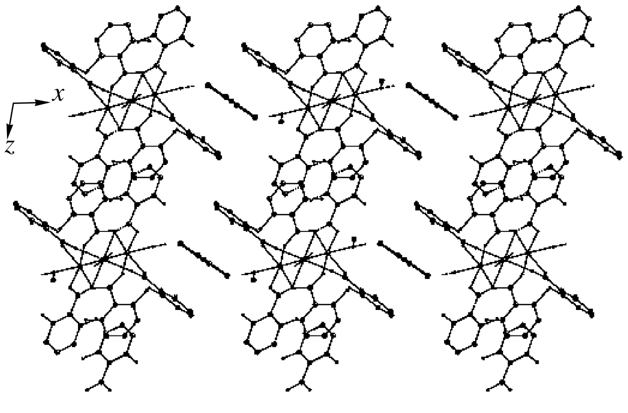

Fig. 3. Fragment of the crystal structure of the complex $[Fe_2CoO(SalH)_6(CH_3OH)_2(H_2O)] \cdot DMF \cdot 2.5H_2O$.

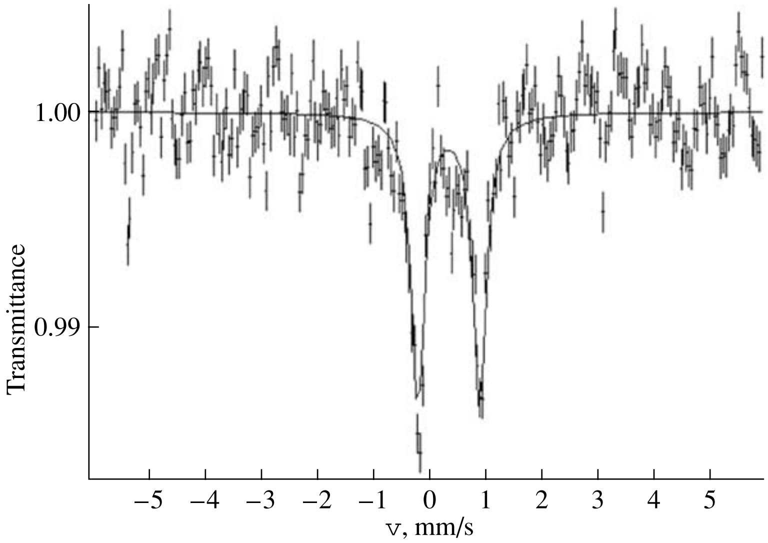

Fig. 4. Mössbauer spectrum of complex **I** at 80 K.

Table 5. Parameters of the Mössbauer spectra of the obtained homo- and heterometallic iron μ_3-oxosalicylates

Complex	T, K	Line width, G	Isomer shift, δ_{Na^+}*	Quadrupole splitting, ΔE_Q	Spin state
		mm/s			
I	300	0.26	0.71	1.08	$S = 5/2$
	80	0.29	0.76	1.28	″
II	300	0.34	0.68	1.04	″
	80	0.32	0.81	1.09	″
$[Fe_2CoO(CH_3COO)_6(3Cl–Py)_3] \cdot n$Solv [34]	300		0.72	0.88	″
	80		0.78	0.97	″
III	300	0.35	0.66	0.76	″

* The isomer shifts are referenced to sodium nitroprusside.

Table 6. Temperature dependence of χ for complex **I**[a]

T, K	χ_{exp}, cm^3/mol	χ^*_{theor}, cm^3/mol	$\chi^* T_{\mathrm{exp}}$, cm K/mol	$\chi^* T_{\mathrm{theor}}$, cm^3 K/mol
291.0000	7697595E-02	7762749E-02	2.240000	2.258960
227.0000	7621145E-02	7599351E-02	1.730000	1.725053
197.0000	7715736E-02	7474888E-02	1.520000	1.472553
175.0000	7314286E-02	7354183E-02	1.280000	1.286982
136.0000	6838235E-02	7038427E-02	0.9300000	0.9572261

[a] $J_{\mathrm{Fe–Fe}} = –44.0$ s^{-1}, $g = 2.05$, the sum of the least squares is = 2.66×10^{-4}.

REFERENCES

1. Kahn, O., *Molecular Magnetism*, New York: Weinheim-Cambridge: VCH, 1993.
2. Harrison, P.M., Hempstead, P.D., Artymiuk, P.J., and Andrews, S.C., *Metal Ions in Biological Systems*, New York: Marcel Dekker, 1998, vol. 35, Ch. 11, p. 435.
3. Long, J.R., *Molecular Cluster Magnets*, Yang., P., Ed., Hong Kong: World Scientific, 2003, p. 291.
4. Sheriff, S., Hendrickson, W.A., and Smith, J.L., *J. Mol. Biol.*, 1987, vol. 197, no. 2, p. 273.
5. Cannon, R.D. and White, R.P., *Prog. Inorg. Chem.*, 1988, vol. 36, p. 196.
6. Cotton, F.A., Extine, M.W., Falvello, L.R., et al., *Inorg. Chem.*, 1986, vol. 25, no. 19, p. 3505.
7. Bond, A.M., Clark, J.H.R., Humphrey, D.G., et al., *Dalton Trans.*, 1998, p. 1845.
8. Ren, X.M., Okudera, H., and Kremer, R.K., *Acta Crystallogr, Sect. E: Structure Reports Online*, 2004, vol. 60, p. 14.
9. Prodius, D.N., *Cand. Sci. (Chem.) Dissertation*, Chisinau: Institute of Chemistry, Moldova Academy of Sciences, 2007.
10. Cui, Y., Zheng, F.K., Yan, D.Ch., et al., *Jiegou Huaxue*, 1998, vol. 17, no. 1, p. 5.
11. Tong, M.L., Wu, Y.L., Chen, X.M., et al., *Chem. Res. Chin. Univ.*, 1998, vol. 14, no. 3, p. 230.
12. Voronkova, V.K., Galeev, R.T., Shova, S., et al., *Appl. Mag. Res.*, 2003, vol. 25, no. 2, p. 227.
13. Tel'zhenskaya, P.N. and Shvarts, E.M., *Koord. Khim.*, 1977, vol. 3, no. 9, p. 1279.
14. Ming-Cai Yin, Chang-Chun Ai, Liang-Jie Yuan, et. al., *J. Mol. Struct.*, 2004, vol. 33, p. 691.
15. Shake, A.R., Tsai, H.L., Webb, R.J., et al., *Inorg. Chem.*, 1994, vol. 33, no. 26, p. 6020.
16. Allen, F.N., *Acta Crystallogr., Sect. B: Struct. Sci.*, 2002, vol. 58, no. 2, p. 380.
17. Otwinowski, Z. and Minor, W., *Methods in Enzymology*, Carter, C.W. and Sweet, R.M., Eds., New York: Academic, 1997, vol. 276, Pt A, p. 276.
18. *XEMP. Version 4.2*, Siemens Analytical X-Ray Inst. Inc., 1990.
19. Sheldrick, G.M., *SHELX-97. Program for Refinement of Crystal Structures*, Göttingen (Germany): Univ. of Göttingen, 1997.
20. Kalinnikov, V.T. and Rakitin, B.V., *Vvedenie v magnetokhimiyu. Metod staticheskoi magnitnoi vospriimchivosti v khimii* (Introduction to Magnetochemistry. The Method of Static Magnetic Susceptibility in Chemistry), Moscow: Mir, 1980.
21. Nakamoto, T., Hanaya, M., Katada, M., *et* al., *Inorg. Chem.*, 1997, vol. 36, p. 4347.
22. Jang, H.G., Geib, S.J., Kaneko, Y., et al., *J. Am. Chem. Soc.*, 1989, vol. 111, p. 173.
23. Woehler, S.E., Wittebort, R.J., Oh, S.M., et al., *J. Am. Chem. Soc.*, 1987, vol. 109, p. 1063.
24. Turta, C.I., Shova, S.G., Prodius, D., et al., *Inorg. Chim. Acta*, 2004, vol. 357, no. 15, p. 4396.
25. Zhang, H.H. and Yu, X.F., *Chin. J. Sruct. Chem. (Jiegou Huaxue)*, 1990, vol. 9, no. 1, p. 1.
26. Batsanov, A.S., Timko, G.A., Struchkov, Yu.T., et al., *Koord. Khim.*, 1991, vol. 17, no. 7, p. 922.
27. Singh, B., Long, J.R., and de Biani, F.F., et al., *J. Am. Chem. Soc.*, 1997, vol. 119, no. 30, p. 7030.
28. Turta, K.I., Shova, S.G., Zhovmir, F.K., et al., *Zh. Neorg. Khim.*, 2003, vol. 48, no. 1, p. 80 [*Russ. J. Inorg. Chem.* (Engl. Transl.), vol. 48, no. 1, p. 72].
29. Prodius, D., Turta, C.I., Mereacre, V.M., et al., *Polyhedron*, 2006, vol. 25, p. 2175.
30. Wells, A.F., *Structural Inorganic Chemistry*, Oxford: Claredent, 1984.
31. Wang, Zh.M. and Yu, X-F., *Chin. J. Sruct. Chem. (Jiegou Huaxue)*, 1990, vol. 9, no. 1, p. 14.
32. Sato, T. and Ambe, F., *Acta Crystallogr., Sect. C: Cryst. Struct. Commun.*, 1996, vol. 52, p. 3005.
33. Nakomoto, K., *Infrared and Raman Spectra of Inorganic and Coordination Compounds*, New York: Wiley, 1986.
34. Zhovmir, T.K., Turta, K.I., Shova, S.G., et al., *Zh. Strukt. Khim.*, 1999, vol. 40, no. 6, p. 1155.
35. Long, G.J., Robinson, W.T., Tappeyer, et al., *J. Chem. Soc., Dalton Trans.*, 1973, no. 6, p. 573.
36. Duncan, J.F., Kanekar, C.R., and Mok, K.F., *J. Chem. Soc., A*, 1969, no. 3, p. 480.
37. Mansurov, M.M., Semenova, G.L., Yakubov, Kh.M., et al., *Zh. Neorg. Khim.*, 1983, vol. 28, no. 6, p. 1460.
38. Yakubov, Kh.M., Semenov, G.L., Mansurov, M.M., *Zh. Neorg. Khim.*, 1985, vol. 30, no. 2, p. 368.
39. Nefed'ev, A.V., Lapkina, N.D., Stukan, R.A., et al., *Zh. Strukt. Khim.*, 1979, vol. 20, no. 5, p. 835.
40. Pound, R.V. and Rebka, G.A., *Phys. Rev. Lett.*, 1960, vol. 4, no. 6, p. 274.
41. Josephson, B.D., *Phys. Rev. Lett.*, 1960, vol. 4, no. 7, p. 341.
42. Van Vleck, J.H., *Theory of Electric and Magnetic Susceptibilities*, London-Oxford: Univ., 1932.